Synthesis and Structural Characterization of Neutral and Cationic Alkylaluminum Complexes Based on Bidentate Aminophenolate Ligands

Samuel Dagorne,*,† Laurent Lavanant,† Richard Welter,‡ Christophe Chassenieux,§ Pierre Haquette,† and Gérard Jaouen†

Laboratoire de Chimie Organométallique, UMR CNRS 7576, Ecole Nationale Supérieure de Chimie de Paris, 11, rue Pierre et Marie Curie, F-75231 Paris Cedex 05, France, Laboratoire DECMET, Institut Le Bel, Université Louis Pasteur, 4, rue Blaise Pascal, 67000 Strasbourg, France, and Laboratoire de Physico-chimie Macromoléculaire, UMR CNRS 7615, Ecole Supérieure de Physique et de Chimie Industrielles, 10, rue Vauquelin, 75231 Paris Cedex 05, France

Received March 21, 2003

The reaction of the aminophenols 2-(CH_2L)-6-R-C_6H_3OH (R = Ph, L = NMe_2, **1a**; R = ^{t}Bu, L = NMe_2, **1b**; R = ^{t}Bu, L = NC_4H_8, **1c**; R = ^{t}Bu, L = NC_5H_{10}, **1d**) with 1 equiv of $AlMe_3$ affords the corresponding dimethyl Al complexes {2-(CH_2L)-6-R-C_6H_3O}$AlMe_2$ (R = Ph, L = NMe_2, **2a**; R = ^{t}Bu, L = NMe_2, **2b**; R = ^{t}Bu, L = NC_4H_8, **2c**; R = ^{t}Bu, L = NC_5H_{10}, **2d**) in high yields. Compounds **2a**−**d** appear to be monomeric, on the basis of X-ray analysis for **2b**,**d** and NMR data for **2a**−**d**, and are stable in the presence of THF. {2-(CH_2NMe_2)-6-Ph-C_6H_3O}$AlMe_2$ (**2a**) cleanly reacts with $B(C_6F_5)_3$ to yield the dinuclear cationic Al species **3a**$^+$. X-ray diffraction analysis shows that the cation **3a**$^+$ can be seen as an adduct of the three-coordinate cation {2-(CH_2NMe_2)-6-Ph-C_6H_3O}$AlMe^+$ and the neutral precursor **2a**, in which the two Al centers are connected via a μ_2-O aminophenolate bridge. Similarly, the reaction of Al dimethyl complexes **2b**−**d** with $B(C_6F_5)_3$ yields dinuclear cationic Al species **3b**−**d**$^+$/**3b′**−**d′**$^+$ (**3b**$^+$/**3b′**$^+$ in a 1/1 ratio; **3c**,**d**$^+$/**3c′**,**d′**$^+$ in a 3/1 ratio, respectively) as diastereomeric mixtures. Cations **3b**−**d**$^+$/**3b′**−**d′**$^+$ adopt a structure similar to that of cation **3a**$^+$, as determined by X-ray crystallography analysis for **3b′**$^+$ and 2D NMR studies for **3a**$^+$ and **3c**,**d**$^+$/**3c′**,**d′**$^+$. All the formed dinuclear cations are quite stable and robust in solution, and no fluxional behavior for any of them was observed up to 80 °C in C_6D_5Br. Cations **3b**−**d**$^+$/**3b′**−**d′**$^+$ react with a Lewis base such as THF to afford the corresponding THF adduct cation **4b**−**d**$^+$ along with 1 equiv of the corresponding neutral precursor **2b**−**d**. In contrast, **3a**$^+$ reacts with THF to yield unidentified species. **3a**$^+$ and **3c**,**d**$^+$/**3c′**,**d′**$^+$ are inactive in ethylene polymerization, but cations **3b**−**d**$^+$/**3b′**−**d′**$^+$ polymerize PO with moderate activity to yield low-molecular-weight PPO.

Introduction

There has recently been an increased interest in cationic aluminum complexes for use in olefin,[1b−e] alkene oxide,[1a,e,2] and (D,L)-lactide[3] polymerization catalysis. These species are interesting, because the enhanced Lewis acidity of the aluminum center versus that of their neutral analogues should yield greater catalytic activity and may allow new applications.[4] In particular, three- and four-coordinate cationic Al alkyls are now attracting attention, since they have been shown to polymerize ethylene under mild conditions.[1c] Such cationic species can be generated by the reaction of Al dialkyl precursors bearing a monoanionic bidentate (LX^-) or tridentate (L_2X^-) ligand with $[Ph_3C][B(C_6F_5)_4]$ or $B(C_6F_5)_3$, via an alkyl abstraction at the metal center.[1c,d]

Whereas the ionization chemistry of neutral Al dialkyls {L_2X}AlR_2 usually generates stable four-coordinate cationic Al species,[1d,5] that of {LX}AlR_2 complexes may yield more reactive three-coordinate Al alkyl cations due to the absence of a second L ligand to stabilize the formed cationic Al center.[6] Thorough studies by Jordan on cationic Al alkyls containing N,N-

* To whom correspondence should be addressed. Fax: +33 1 43 26 00 61. E-mail: dagorne@ext.jussieu.fr.
† Ecole Nationale Supérieure de Chimie de Paris.
‡ Université Louis Pasteur.
§ Ecole Supérieure de Physique et de Chimie Industrielles.

(1) For key references, see: (a) Atwood, D. A.; Jegier, J. A.; Rutherford, D. *J. Am. Chem. Soc.* **1995**, *117*, 6779. (b) Bochmann, M.; Dawson, D. M. *Angew. Chem., Int. Ed. Engl.* **1996**, *35*, 2226. (c) Coles, M. P.; Jordan, R. F. *J. Am. Chem. Soc.* **1997**, *119*, 8125. (d) Bruce, M.; Gibson, V. C.; Redshaw, C.; Solan, G. A.; White, A. J. P.; Williams, D. J. *Chem. Commun.* **1998**, 2523. (e) Kim, K.-C.; Reed, C. A.; Long, G. S.; Sen, A. *J. Am. Chem. Soc.* **2002**, *124*, 7662.

(2) (a) Jegier, J. A.; Atwood, D. A. *Inorg. Chem.* **1997**, *36*, 2034. (b) Munoz-Hernandez, M.-A.; Sannigrahi, B.; Atwood, D. A. *J. Am. Chem. Soc.* **1999**, *121*, 6747.

(3) Emig, N.; Nguyen, H.; Krautscheid, H.; Réau, R.; Cazaux, J.-B.; Bertrand, G. *Organometallics* **1998**, *17*, 3599.

(4) Atwood, D. A. *Coord. Chem. Rev.* **1998**, *176*, 407.

(5) (a) Cameron, P.; Gibson, V. C.; Redshaw, C.; Segal, J. A.; Bruce, M. D.; White, A. J. P.; Williams, D. J. *Chem. Commun.* **1999**, 1883. (b) Cameron, P.; Gibson, V. C.; Redshaw, C.; Segal, J. A.; Bruce, M. D.; White, A. J. P.; Williams, D. J. *J. Chem. Soc., Dalton Trans.* **2002**, 415.

10.1021/om0302185 CCC: $25.00
Publication on Web 08/02/2003

Chart 1

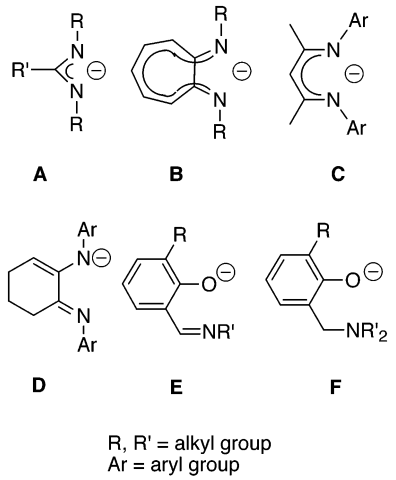

Scheme 1

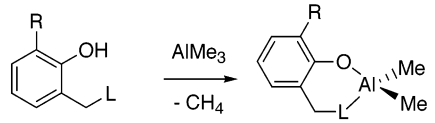

1a: R = Ph, L = NMe_2
1b: R = ^{t}Bu, L = NMe_2
1c: R = ^{t}Bu, L = NC_4H_8
1d: R = ^{t}Bu, L = NC_5H_{10}

bidentate systems (**A**−**C**; Chart 1) showed that the structure of these species, their stability, and their reactivity are strongly influenced by the nature of the ancillary ligand.[6,7] In particular, the design of the chelating N,N-bidentate ligand strongly affects the catalytic activity of the derived cations.

In contrast to the N,N-ligand systems (**A**−**D**; Chart 1),[6,7,8] O,N-bidentate cationic Al complexes have received much less attention, with the exception of recent reports on the ionization chemistry of Al dialkyl complexes containing one mono(iminophenolate) ligand (**E**; Chart 1), which yielded unstable cations in the absence of an external Lewis base.[5a,8b,9]

Our attention focused on the synthesis of stable and well-defined O,N-bidentate Al alkyl cations, because such species may be structurally interesting as well as useful for catalytic purposes. Bidentate O,N-aminophenolate ligands (**F**; Chart 1) seemed suitable for our studies, since they may constitute an excellent chelate for the oxophilic Al center and may form a stable, while still flexible, six-membered Al metallacycle. Aluminum phenolates without sterically demanding ortho substituents are known to readily form aggregates.[10] Thus, to limit association reactions, we focused our studies on the use of di-ortho-substituted aminophenols. Overall, the geometrical and electronic differences between **F** and **A**−**E** may be reflected in the structure and the reactivity of the obtained cationic Al alkyls. Here we report the synthesis and structure of neutral and cationic aluminum complexes incorporating aminophenolate ligands of type **F**. The newly synthesized cationic species have also been tested for polymerization activity.

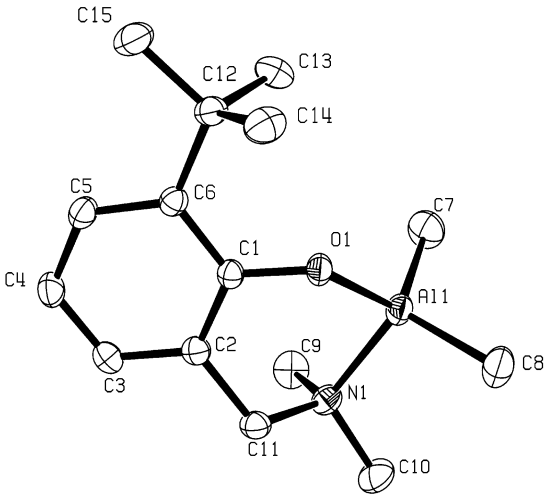

Figure 1. Molecular structure of complex **2b**. The H atoms are omitted for clarity. Selected bond lengths (Å) and angles (deg): Al(1)−O(1) = 1.758(1), Al(1)−N(1) = 2.036(1), Al(1)−C(7) = 1.956(2), Al(1)−C(8) = 1.954(2); O(1)−Al(1)−C(8) = 109.95(7), O(1)−Al(1)−C(7) = 112.94(6), C(8)−Al(1)−C(7) = 118.13(7), O(1)−Al(1)−N(1) = 97.17(5), C(8)−Al(1)−N(1) = 108.67(6), C(7)−Al(1)−N(1) = 107.81(7). Selected torsion angles (deg): Al(1)−O(1)−C(1)−C(2) = 39.29(16), O(1)−C(1)−C(2)−C(11) = 3.13(18), N(1)−C(11)−O(1)−Al(1) = 23.21(9).

Results

Synthesis and Structure of Mono(aminophenolate) Al Dimethyl Complexes. The reaction of aminophenols **1a**−**d** with 1 equiv of $AlMe_3$ in pentane at 0 °C affords the corresponding Al dimethyl complexes {2-(CH_2L)-6-R-C_6H_3O}$AlMe_2$ (R = Ph, L = NMe_2, **2a**; R = ^{t}Bu, L = NMe_2, **2b**; R = ^{t}Bu, L = NC_4H_8, **2c**; R = ^{t}Bu, L = NC_5H_{10}, **2d**; Scheme 1) as analytically pure colorless solids in high yields. X-ray-quality crystals of **2b** and **2d** were obtained from a saturated Et_2O solution, and the molecular structures of both compounds were determined by X-ray crystallographic analysis, establishing their monomeric nature. The molecular structures of **2b**,**d** and their selected bond distances and angles are shown respectively in Figures 1 and 2, and crystallographic data are given in Table 1. Compounds **2b**,**d** exhibit very similar structural features, and thus, we will discuss only the features for **2d**.

Compound **2d** crystallizes as a monomer in which the Al center adopts a slightly distorted tetrahedral geometry. The bite angle of the η^2(O,N)-bonded aminophe-

(6) (a) Ihara, E.; Young, V. G., Jr.; Jordan, R. F. *J. Am. Chem. Soc.* **1998**, *120*, 8277. (b) Radzewich, C. E.; Guzei, I. A.; Jordan, R. F. *J. Am. Chem. Soc.* **1999**, *121*, 8673.

(7) (a) Radzewich, C. E.; Coles, M. P.; Jordan, R. F. *J. Am. Chem. Soc.* **1998**, *120*, 8673. (b) Dagorne, S.; Guzei, I. A.; Coles, M. P.; Jordan, R. F. *J. Am. Chem. Soc.* **2000**, *122*, 274. (c) Korolev, A. V.; Ihara, E.; Guzei, I. A.; Young, V. G., Jr.; Jordan, R. F. *J. Am. Chem. Soc.* **2001**, *122*, 274.

(8) (a) Schmidt, J. A. R.; Arnold, J. *Organometallics* **2002**, *21*, 2306. (b) Pappalardo, D.; Tedesco, C.; Pellecchia, C. *Eur. J. Inorg. Chem.* **2002**, 621.

(9) Cameron, P.; Gibson, V. C.; Redshaw, C.; Segal, J. A.; Solan, G. A.; White, A. J. P.; Williams, D. J. *J. Chem. Soc., Dalton Trans.* **2001**, 1472.

(10) (a) Pasynkiewicz, S.; Starowieyski, K. B.; Skowronska-Ptasinska, M. *J. Organomet. Chem.* **1973**, *52*, 269. (b) Starowieyski, K. B.; Skowronska-Ptasinska, M. *J. Organomet. Chem.* **1978**, *157*, 379. For a review on sterically crowded aryloxide compounds of aluminum, see: (c) Healy, M. D.; Power, M. B.; Barron, A. R. *Coord. Chem. Rev.* **1994**, *130*, 63.

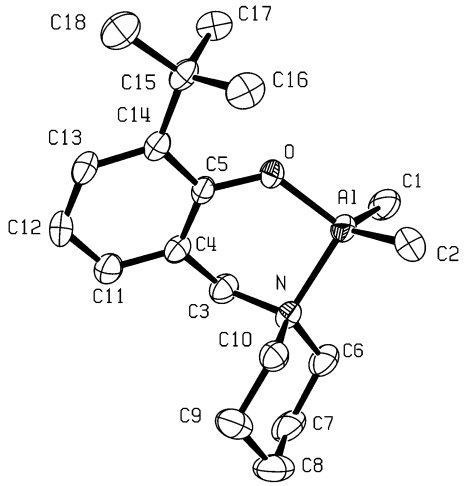

Figure 2. Molecular structure of complex **2d**. The H atoms are omitted for clarity. Selected bond lengths (Å) and angles (deg): Al−O = 1.768(2), Al−N = 2.019(2), Al−C(1) = 1.957(3), Al−C(2) = 1.954(3); O−Al−C(1) = 113.3(1), O−Al−C(2) = 108.5(1), C(1)−Al−C(2) = 116.4(1), O−Al−N = 96.81(9), C(2)−Al−N = 108.5(1), C(1)−Al−N = 107.2(1). Selected torsion angles (deg): Al−O−C(4)−C(5) = 11.9, O(1)−C(1)−C(2)−C(11) = 3.13(18), N−C(3)−O−Al = 35.9, C(4)−C(3)−O−C(5) = 2.5.

nolate (N−Al−O = 96.81(9)°) is compensated by the opening of the C(1)−Al−C(2) and O−Al−C bond angles (average 116.4(1) and 112.9°, respectively). The N−Al−C bond angles (107.9(7)°) are very close to the ideal tetrahedral angle (109.49°). The six-membered-ring Al metallacycle is puckered, with the Me_2N−Al moiety well above the nearly planar O−C(5)−C(4)−C(3) backbone, as shown by the C(5)−C(4)−C(3)−N and O−Al−N−C(3) torsion angles (56.0 and 47.6°, respectively). Similar puckering was also observed in the related boron analogue {2-(CH_2NMe_2)C_6H_4O}BPh_2.[11] The Al−O and Al−N bond distances (1.768(2) and 2.019(2) Å, respectively) are in the normal range found for aluminum phenolates (1.640(5)−1.773(2) Å)[10c,12] and for Al−N dative bonds (1.957(3)−2.238(4) Å),[13] respectively.

The NMR data for **2a**−**d** are consistent with the chelation of one aminophenolate ligand to the Al center and with the solid-state structure being retained in solution. These data also show an effective C_s symmetry for **2a**−**d** on the NMR time scale in C_6D_6 at room temperature, which is most likely due to a fast conformation change of the six-membered-ring Al metallacycle under these conditions, as observed in solution for {2-(CH_2NMe_2)C_6H_4O}BPh_2.[11] No reaction was observed between **2a**−**d** and THF (1 equiv) after 2 days at 70 °C in C_6D_6. This contrasts with the lack of stability of {2-(CH_2NMe_2)C_6H_4O}$AlMe_2$ in the presence of such a Lewis base, which undergoes a disproportionation reaction to yield {2-(CH_2NMe_2)C_6H_4O}$_2$AlMe and THF−$AlMe_3$.[12] Such different reactivity may be ascribed to the more sterically demanding aminophenolate in **2a**−**d**.

Synthesis and Structure of Cationic Al Alkyls Derived from Complexes 2a−d. Reaction of {2-(CH_2NMe_2)-6-Ph-C_6H_3O}$AlMe_2$ (2a) with $B(C_6F_5)_3$. The reaction of the Al dimethyl compound {2-(CH_2-NMe_2)-6-Ph-C_6H_3O}$AlMe_2$ (**2a**) with 1 equiv of $B(C_6F_5)_3$ in CD_2Cl_2 (30 min, room temperature) cleanly affords the dinuclear cations [{2-(CH_2NMe_2)-6-Ph-C_6H_3O}-AlMe·{2-(CH_2NMe_2)-6-Ph-C_6H_3O}$AlMe_2$]$^+$ (**3a**$^+$) as $MeB(C_6F_5)_3^-$ salts (100% conversion by ^{1}H NMR; Scheme 2), along with 0.5 equiv of unreacted $B(C_6F_5)_3$, as observed by ^{19}F NMR. This reaction generates the dinuclear species **3a**$^+$, which contains two elements of chirality: i.e., a stereogenic tetrahedral Al center and a second element of chirality resulting from the configurational stability of the $AlMe_2$ chelate ring.[14] Thus, two diastereomers are a priori expected. In this case, the reaction is diastereoselective at room temperature (>96% by ^{1}H NMR), since only cation **3a**$^+$ is observed. The salt [**3a**][$MeB(C_6F_5)_3$] is stable in CD_2Cl_2 at room temperature for several days and was isolated as an analytically pure colorless solid in 76% yield by generation in CH_2Cl_2, removal of volatiles, and pentane washing. X-ray-quality crystals of [**3a**][$MeB(C_6F_5)_3$] were grown from a saturated 10/1 CH_2Cl_2/pentane solvent mixture at room temperature and its molecular structure was determined by X-ray crystallography analysis.

Molecular Structure of [3a][MeB(C_6F_5)$_3$]. [**3a**]-[$MeB(C_6F_5)_3$] crystallizes as discrete **3a**$^+$ (Figure 3) and $MeB(C_6F_5)_3^-$ ions with no close cation−anion contacts. The structure of $MeB(C_6F_5)_3^-$ is normal. The molecular structure of **3a**$^+$ is shown in Figure 3, crystallographic data are given in Table 1, and selected bond distances and angles are summarized in Table 2. It has an overall C_1 symmetry structure and can be seen as an adduct of the three-coordinate cation {2-(CH_2NMe_2)-6-Ph-C_6H_3O}-AlMe$^+$ and the neutral four-coordinate complex {2-(CH_2-NMe_2)-6-Ph-C_6H_3O}$AlMe_2$, in which the two Al centers are linked by a μ_2-O bridging aminophenolate ligand through O(2). A related cationic Al dinuclear adduct, but containing a μ_2-amido bridge, was observed in the ionization chemistry of the amidinate complex {^{t}BuC-(N^iPr)$_2$}$AlMe_2$; this adduct was revealed to be unstable and could not be fully characterized.[7b]

The geometrical parameters at the Al centers for **3a**$^+$ are nearly unchanged as compared to those of the neutral precursors. Both Al centers adopt a slightly distorted tetrahedral structure with N−Al−O bite angles (N(1)−Al(1)−O(1) = 99.16° and N(2)−Al(2)−O(2) = 96.07°) similar to those of **2b**,**d** (average 96.9(2)°).

The presence of two aminophenolate ligands in a different binding mode is clearly manifest through their geometrical differences. As shown in Figure 2, the six-membered-ring Al(1) metallacycle is slightly puckered, with Al(1) and N(1) slightly outside of the rest of the ring. In contrast, the six-membered-ring Al(2) metallacycle containing the bridging aminophenolate adopts a boatlike conformation with the O(2) and C(21) well above the Al(2)−N(2)−C(21)−C(22) backbone, which

(11) Hagen, H.; Reinoso, S.; Albrecht, M.; Boersma, J.; Spek, A. L.; van Koten, G. *J. Organomet. Chem.* **2000**, *608*, 27.

(12) Hogerheide, M. P.; Wesseling, M.; Jastrzebski, J. T. B. H.; Boersma, J.; Kooijman, H.; Spek, A. L.; van Koten, G. *Organometallics* **1995**, *14*, 4483.

(13) (a) Hill, J. B.; Eng, S. J.; Pennington, W. T.; Robinson, G. H. *J. Organomet. Chem.* **1993**, *445*, 11. (b) Kumar, R.; Sierra, M. L.; Oliver, J. P. *Organometallics* **1994**, *13*, 4285.

(14) The obtainment in solution of two diastereomers in the **3b**−**d**$^+$/**3b**′−**d**′$^+$ cationic systems (vide infra) imposes the presence of a second element of chirality for these cations. This second source of chirality most likely originates from a configurationally stable (i.e. with no inversion) $AlMe_2$ chelate ring in all the obtained dinuclear cations. This feature is proposed on the basis of the solid-state structure studies of **3a**$^+$ and **3b**′$^+$ and of the lack of dynamic behavior in solution for **3a**$^+$ and **3b**−**d**$^+$/**3b**′−**d**′$^+$ (vide infra).

Table 1. Crystallographic Data for 2b,d, [3a][MeB(C_6F_5)], and [3b′][MeB(C_6F_5)]

	2b	2d	[**3a**][MeB(C_6F_5)]	[**3b′**][MeB(C_6F_5]
formula	4($C_{15}H_{26}AlNO$)	$C_{18}H_{30}AlNO$	$C_{52}H_{44}Al_2BF_{15}N_2O_2$	$C_{48}H_{52}Al_2BF_{15}N_2O_2$
fw	1053.39	303.43	1078.69	1038.71
cryst size (mm)	0.13 × 0.10 × 0.08	0.20 × 0.10 × 0.08	0.11 × 0.09 × 0.06	0.10 × 0.08 × 0.06
cryst syst	triclinic	monoclinic	triclinic	monoclinic
space group	$P\bar{1}$	$P2_1/c$	$P\bar{1}$	$P2_1/c$
a (Å)	10.310(5)	9.7860(3)	10.1644(2)	16.8813(2)
b (Å)	12.692(5)	10.2945(4)	16.1355(2)	11.1788(1)
c (Å)	25.691(5)	18.1648(7)	16.6117(3)	25.4984(4)
α (deg)	78.056	90	114.004(5)	90
β (deg)	80.587(5)	96.603(5)	91.562(5)	90.479
γ (deg)	87.421(5)	90	93.640(5)	90
V (Å^3)	3245(2)	1817.8(1)	2479.59(12)	4811.7(1)
Z	2	4	2	4
D_{calcd} (g cm^{-3})	not measd	1.11	1.44	1.43
no. of indep rflns	17223	4223		13331
no. of params	649	190	667	631
R1	0.051[a]	0.045[b]	0.043[b]	0.042[b]
wR2 (all data)	0.1508	0.123		0.227
goodness of fit	1.050	1.068	1.154	1.134

[a] R1 ($I > 2\sigma(I)$). [b] R1 ($I > 3\sigma(I)$).

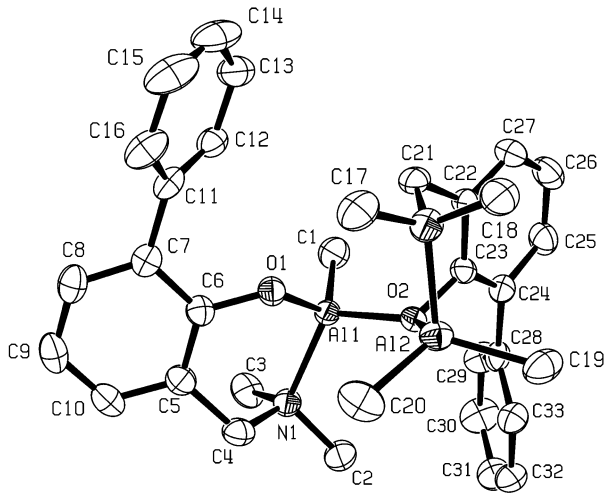

Figure 3. Molecular structure of complex **3a**$^+$. The H atoms are omitted for clarity.

Scheme 2

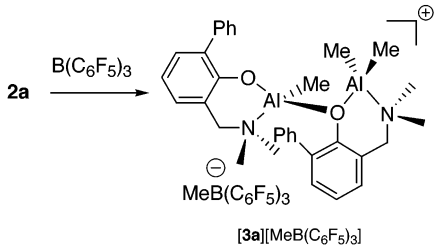

illustrates the flexibility of this ligand. Such a conformation can be rationalized by the geometrical restraints imposed on the aminophenolate ligand by both the coordination of O(2) to Al(1) and the tetrahedral geometry preferred by Al(2).

The coordination of the O(2) to both Al centers leads to a slightly distorted trigonal planar geometry around O(2), the sum of the angles amounting to 350.3(4)° (O(2) is 0.31(1) Å out of the plane defined by Al(1), Al(2), and C(23)). In comparison to the geometry around the oxygen in **2b**,**d**, this can be seen as a rehybridization from sp^3 to sp^2 caused by the coordination of O(2) to Al(1). The Al(1)−O(2) bond distance is shorter than the Al(2)−O(2) bond distance (1.846(1) and 1.881(2) Å,

Table 2. Selected Bond Lengths (Å) and Angles (deg) for 3a$^+$

Al(1)−O(1)	1.729(2)	Al(1)−O(2)	1.846(1)
Al(1)−N(1)	1.975(2)	Al(1)−C(1)	1.926(3)
Al(2)−O(2)	1.881(2)	Al(2)−N(2)	2.020(2)
Al(2)−C(19)	1.948(3)	Al(2)−C(20)	1.936(3)
Al(1)−O(2)−Al(2)	129.24(8)	N(2)−Al(2)−O(2)	96.09
N(1)−Al(1)−O(1)	99.16(8)	Al(1)−O(2)−C(23)	112.4(1)
Al(2)−O(2)−C(23)	108.7(1)	N(1)−Al(1)−O(2)	114.02(7)
O(2)−Al(1)−C(1)	111.39(9)	O(2)−Al(2)−C(20)	112.7(1)
O(2)−Al(2)−C(19)	110.1(1)	C(20)−Al(2)−C(19)	116.2(1)
N(2)−Al(2)−C(20)	111.4(1)	N(2)−Al(2)−C(19)	108.6(1)
N(1)−Al(1)−C(1)	111.9(1)	O(1)−Al(1)−C(1)	120.4(1)

Chart 2

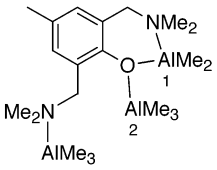

G

respectively), but both distances compare to those in $Et_2Al(\mu\text{-O-2,6-}Me_2Ph)_2AlEt_2$ (average 1.86(1) Å), which shows the bridging phenoxide nature of the O(2) group.[15] The similar *μ*-O−Al bond distances in **3a**$^+$ contrast with the different values of the Al(1)−O and Al(2)−O bond distances (1.855(2) and 1.989(2) Å, respectively) in a related neutral trinuclear complex (**G**; Chart 2).[12] The more symmetrical phenoxide Al−O−Al bridge in our case may be ascribed to the electron deficiency of both Al centers as a result of the cationic charge. The Al(1)−N(1) bond distance (1.975(1) Å) is shorter than the Al(2)−N(2) distance (2.020(2) Å), the latter being identical with that in **2d** (2.019(2) Å), while both remain in the normal range for Al−N dative bonds (1.957(3)−2.238(4) Å).[12,13] Overall, the shorter Al(1)−N and Al(1)−O bond distances as compared to the Al(2)−N and Al(2)−O bond distances in **3a**$^+$ may suggest a more electron-deficient Al(1) vs Al(2).

Solution Structure and Stability of [3a][MeB(C_6F_5)$_3$]. The solution structure of [**3a**][MeB(C_6F_5)$_3$] was

(15) Giesbrecht, G. R.; Gordon, J. C.; Brady, J. T.; Clark, D. L.; Webster Keogh, D.; Michalczyk, R.; Scott, B. L.; Watkin, J. G. *Eur. J. Inorg. Chem.* **2002**, 723.

Scheme 3

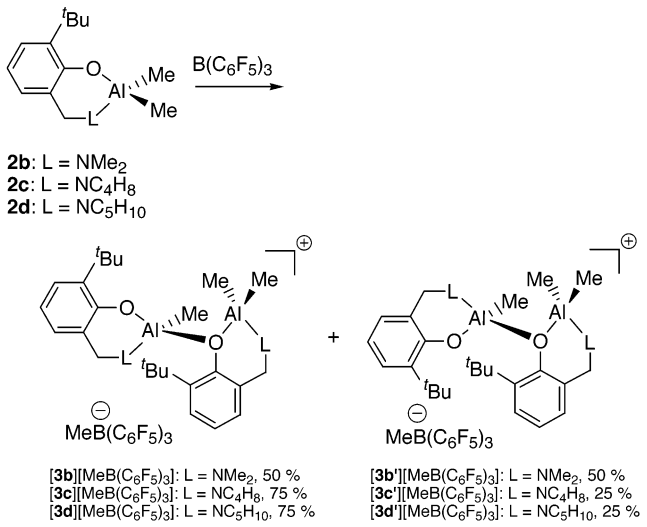

studied by a combination of 1D (^{1}H, ^{11}B, ^{13}C, and ^{19}F NMR) and 2D (HMQC and HMBC) NMR spectroscopy techniques, which allowed a complete assignment for all resonances.

The ^{1}H, ^{11}B, ^{13}C, and ^{19}F NMR data for [**3a**][MeB(C_6F_5)$_3$] between −40 and +40 °C in CD_2Cl_2 are essentially unchanged, showing that the MeB(C_6F_5)$_3^-$ anion is free in solution and that the cation **3a**$^+$ is not fluxional over this range of temperature. Similar NMR data are obtained for [**3a**][MeB(C_6F_5)$_3$] in C_6D_5Br between −10 and +80 °C in C_6D_5Br. However, cation **3a**$^+$ decomposes at 90 °C in C_6D_5Br ($t_{1/2} \approx$ 3h) to unidentified species. In addition, the ^{1}H NMR spectrum of **3a**$^+$ also remains unchanged in the presence of the neutral precursor **2a** (1 equiv) between 25 and 80 °C in C_6D_5Br showing that no exchange reaction occurs between the two species under such conditions.

The ^{1}H and ^{13}C NMR data for **3a**$^+$ are consistent with a C_1-symmetric structure in solution. For example, the ^{1}H spectrum for **3a**$^+$ at 35 °C contains 3 Al*Me* resonances, 4 N*Me* signals, 4 PhCH_2 resonances, and two sets of aminophenolate resonances in the aromatic region. In addition, the atomic connectivity for **3a**$^+$ established on the basis of HMQC and HMBC NMR experiments is consistent with the solid-state structure. Overall, the NMR data for **3a**$^+$ strongly suggest that its solid-state structure is retained in solution.

Reaction of Dimethyl Al Complexes 2b−d with B(C_6F_5)$_3$. The ionization chemistry of neutral precursors incorporating bulkier aminophenolates (**2b−d**) was studied in order to probe the influence of the aminophenolate sterics on the structure and the nature of the formed Al alkyl cations. As described below, the change from a Ph ortho substituent in **2a** to a ^{t}Bu ortho substituent in **2b−d** does not affect the overall structure of the formed cations but does affect the diastereoselectivity.

The compounds {2-(CH_2L)-6-^{t}Bu-C_6H_3O}AlMe$_2$ (L = NMe$_2$, **2b**; L = NC_4H_8, **2c**; L = NC_5H_{10}, **2d**; Scheme 3) react with B(C_6F_5)$_3$ to yield the corresponding dinuclear cations [{2-(CH_2L)-6-^{t}Bu-C_6H_3O}AlMe·{{2-(CH_2L)-6-^{t}Bu-C_6H_3O}AlMe$_2$]$^+$ (**3b−d**$^+$/**3b′−d′**$^+$) as a mixture of two diastereomers and as MeB(C_6F_5)$_3^-$ salts (**3b**$^+$/**3b′**$^+$ in a 1/1 ratio; **3c**,**d**$^+$/**3c′**,**d′**$^+$ in a 3/1 ratio, respectively, 100% conversion by ^{1}H NMR; Scheme 3), along with 0.5 equiv of unreacted B(C_6F_5)$_3$ as observed by ^{19}F NMR. Thus, the diastereoselectivity of this reaction is significantly lower than that with **2a** and appears to be highly influenced by the steric nature of the aminophenolate ligand. The different diastereomeric ratios of **3a**$^+$ vs **3b**$^+$/**3b′**$^+$ and of **3b**$^+$/**3b′**$^+$ vs **3c**,**d**$^+$/**3c′**,**d′**$^+$ show that both the phenol and the amino groups influence the diastereoselectivity of these reactions.

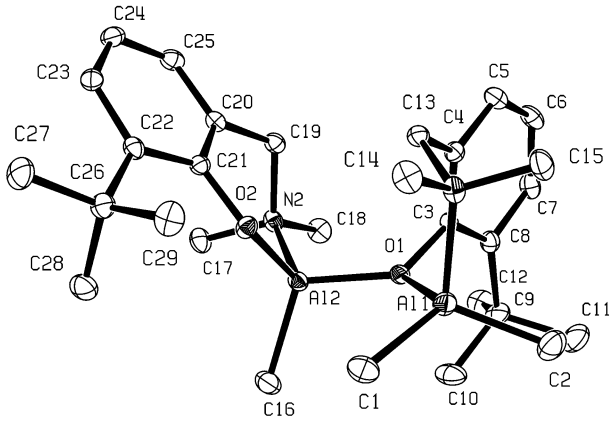

Figure 4. Molecular structure of complex **3b′**$^+$. The H atoms are omitted for clarity.

Table 3. Selected Bond Lengths (Å) and Angles (deg) for 3b′$^+$

Al(2)−O(2)	1.736(2)	Al(2)−O(1)	1.855(2)
Al(2)−N(2)	1.983(2)	Al(2)−C(16)	1.934(2)
Al(1)−O(1)	1.885(2)	Al(1)−N(1)	2.019(2)
Al(1)−C(2)	1.941(3)	Al(1)−C(1)	1.943(3)
Al(1)−O(1)−Al(2)	121.69(8)	N(1)−Al(1)−O(1)	95.72(7)
N(2)−Al(2)−O(2)	95.97(8)	Al(2)−O(1)−C(3)	125.4(1)
Al(1)−O(1)−C(3)	107.7(1)	N(2)−Al(2)−O(1)	111.77(7)
O(1)−Al(2)−C(16)	111.5(1)	O(1)−Al(1)−C(1)	106.46(9)
O(1)−Al(1)−C(2)	112.5(1)	C(1)−Al(1)−C(2)	119.4(1)
N(1)−Al(1)−C(1)	112.6(1)	N(1)−Al(1)−C(2)	107.7(1)
N(2)−Al(2)−C(16)	110.5(1)	O(2)−Al(2)−C(16)	118.07(9)

[**3b−d**/**3b′−d′**][MeB(C_6F_5)$_3$] were isolated at room temperature as diastereomeric mixtures as analytically pure colorless solids in good yields, using a procedure similar to that for [**3a**][MeB(C_6F_5)$_3$]. Crystals of [**3b′**][MeB(C_6F_5)$_3$] were obtained from a 5/1 pentane/CH_2Cl_2 saturated solution, and its molecular structure was determined by X-ray crystallographic analysis. The molecular structure of **3b′**$^+$ is illustrated in Figure 4, crystallographic data are given in Table 1, and selected bond distances and angles are shown in Table 3. Cation **3b′**$^+$ adopts a structure similar to that of **3a**$^+$ and is a formal adduct of {6-^{t}Bu-2-(CH_2NMe$_2$)C_6H_3O}AlMe$^+$ and the neutral four-coordinate complex {2-^{t}Bu-6-(CH_2NMe$_2$)C_6H_3O}AlMe$_2$ linked by a μ_2-O aminophenolate ligand through O(2). However, the stereogenic Al center in **3b′**$^+$ adopts a configuration opposite to that in **3a**$^+$, whereas the AlMe$_2$ chelate ring adopts the same configuration as that in **3a**$^+$. This key stereochemical difference between the molecular structures of **3a**$^+$ and **3b′**$^+$ explains the presence of two diastereomers in **3b−d**$^+$/**3b′−d′**$^+$. Overall, the structural and geometrical parameters for **3b′**$^+$ are similar to those of **3a**$^+$, showing that the presence of the more bulky ^{t}Bu ortho substituent vs a Ph ortho substituent in **3a**$^+$ does not provide enough steric shielding to prevent association.

Solution Structure of [3b−d⁺/3b′−d′][MeB(C₆F₅)₃]. The solution structure of [**3b**−**d**/**3b′**−**d′**][$MeB(C_6F_5)_3$] was studied by a combination of 1D (^1H, ^{11}B, ^{13}C, and ^{19}F NMR) and 2D (HMQC and HMBC) NMR techniques, which allowed a complete assignment for all resonances and connectivity assignments for cations **3b**$^+$ and **3c**,**d**$^+$/**3c′**,**d′**$^+$. The combined 1D and 2D NMR data show the following. (i) The cation and the anion are fully dissociated in CD_2Cl_2 solution between −80 and 35 °C and between room temperature and 70 °C in C_6D_5Br. (ii) Each cation remains C_1 symmetric with no fluxional behavior under the studied conditions. (iii) The diastereomeric ratios **3b**−**d**$^+$/**3b′**−**d′**$^+$ are not modified over the studied range of temperature, which suggests that the reaction is under kinetic control and shows that the Al stereogenic center and the $AlMe_2$ chelate ring are configurationally stable under these conditions.

In addition to 1D and 2D NMR connectivity assignments, a close analysis of the ^{13}C NMR data for **3b**−**d**$^+$/**3b′**−**d′**$^+$ favors the proposed μ_2-O bridging structure of these cations in solution. In particular, for each of these cations, the C(2) and C(4) phenol carbons resonances of the μ_2-O aminophenolate are significantly deshielded as compared to the corresponding resonances of the second aminophenolate ligand. In contrast, the C(1) phenol resonance of the μ-O-aminophenolate in **3b**−**d**$^+$/**3b′**−**d′**$^+$ is shielded as compared to those of the other aminophenolate.[16] These two observations show that the μ-O phenol ring is significantly more electron-deficient than the other phenol ring, as expected for this type of structure. Overall, the NMR data for cations **3b**−**d**$^+$/**3b′**−**d′**$^+$ suggest that they all adopt a structure in solution similar to that of **3b′**$^+$ in the solid state and that, like **3a**$^+$, cations **3c**,**d**$^+$/**3c′**,**d′**$^+$ are quite robust in solution.

In the case of cations **3c**,**d**$^+$/**3c′**,**d′**$^+$, 2D NMR data, including NOESY data, remained inconclusive as to the determination of **3c**$^+$ and **3d**$^+$ as the major diastereomers. Rather, the comparison of ^1H NMR Al*Me* resonances of **3c**,**d**$^+$/**3c′**,**d′**$^+$ to those of **3b**/**3b′**$^+$ provided insight into this issue.[17] The ^1H NMR Al*Me* sets of resonances for **3b**$^+$, **3c**$^+$, and **3d**$^+$ are almost identical but exhibit chemical shifts quite different from those, also very similar to one another, for **3b′**$^+$, **3c′**$^+$, and **3d′**$^+$.[18] This key difference allowed NMR assignments for cations **3c**$^+$ and **3d**$^+$.

Decomposition of [3b/3b′][MeB(C₆F₅)₃] in solution. The stability of the **3b**$^+$/**3b′**$^+$ diastereomeric mixture (1/1 ratio) as $MeB(C_6F_5)_3^-$ salts was studied in C_6D_5Br on an NMR scale. Complete conversion of [**3b**/**3b′**][$MeB(C_6F_5)_3$] to a 1/1/1 ratio of the neutral monomethyl complex {2-(CH_2NMe_2)-6-^{t}Bu-C_6H_3O}Al(Me)(C_6F_5) (**5b**), complex **2b**, and three-coordinated borane $MeB(C_6F_5)_2$ was observed after 5 h at 80 °C in C_6D_5Br (Scheme 4). A preparative-scale synthesis of **5b** by heating [**3b**/**3b′**][$MeB(C_6F_5)_3$] in benzene for 18 h allowed it to be obtained as an analytically pure solid after recrystallization from pentane. The ^1H and ^{13}C NMR data for **5b** are consistent with a C_1-symmetric structure and the ^{19}F NMR data with the presence of the C_6F_5 moiety. The NMR data for $MeB(C_6F_5)_2$ match those of the literature.[19] Similar degradation reactions between cationic Al alkyl systems incorporating bidentate ligands and the $MeB(C_6F_5)_3^-$ anion occurring via a $C_6F_5^-$ transfer from the anion to the Al center have previously been observed.[7b,19] However, degradations of this type usually take place at a temperature lower than that observed here for **3b**$^+$/**3b′**$^+$, thus illustrating the excellent stability of the **3b**$^+$/**3b′**$^+$ system.

Scheme 4

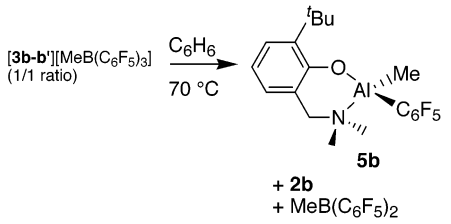

Scheme 5

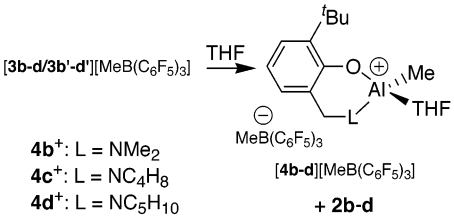

Reaction of Al Cations [3a][MeB(C₆F₅)₃], [3b−d⁺/3b′−d′][MeB(C₆F₅)₃] with THF. The reactivity of the obtained dinuclear cations with a Lewis base such as THF was investigated. The NMR scale reaction of [**3b**−**d**/**3b′**−**d′**][$MeB(C_6F_5)_3$] with 1 equiv of THF in CD_2Cl_2 at room temperature results in quantitative conversion to the cationic THF adduct Al alkyl complexes [**4b**−**d**][$MeB(C_6F_5)_3$] and the neutral precursors **2b**−**d** in a 1/1 ratio, as observed by ^1H NMR (Scheme 5). Attempts to isolate [**4b**−**d**][$MeB(C_6F_5)_3$] by their generation on a preparative scale remained unsuccessful due to their oily nature. In contrast to that of [**4b**−**d**][$MeB(C_6F_5)_3$], the reaction of [**3a**][$MeB(C_6F_5)_3$] with THF in CD_2Cl_2 at room temperature yields unidentified species. When this reaction was performed at −40 °C, a similar intractable mixture was obtained.

Compounds [**4b**−**d**][$MeB(C_6F_5)_3$] are fully dissociated in CD_2Cl_2 with no cation−anion interaction at room temperature, as observed by ^1H and ^{19}F NMR spectroscopy. Key characteristic ^1H NMR resonances for **4b**−**d**$^+$ include (i) the $AlMe^+$ resonances (δ −0.33, −0.37, −0.27 for **4b**−**d**$^+$, respectively) are downfield shifted as compared to those in the neutral precursors (δ −0.76, −0.77, −0.73 respectively), a result of the cationic charge on the Al center, and (ii) the THF resonances (δ (average) 4.44, 2.23) also appear at significantly lower field than those for free THF (δ 3.67, 1.81), showing effective THF coordination to the cationic Al center. The ^{13}C NMR data for **4b**−**d**$^+$ exhibit a

(16) For the μ-O aminophenolate: δ (average) 126.8 (C′(2)), 127.6 (C′(4)), 146.5 (C′(1)). For the other aminophenolate: δ (average) 120.7 (C(2)), 119.9 (C(4)), 154.7 (C(1)). For more details, see the Experimental Section.

(17) The NMR data of the single crystals obtained from slow crystallization of [**3b**$^+$/**3b′**][$MeB(C_6F_5)_3$] (1/1 ratio) from solution contain signals for only one diastereomer, which were assigned to cation **3b′**$^+$ on the basis of X-ray crystallographic results.

(18) ^1H NMR Al*Me* resonances (CD_2Cl_2): **3b**$^+$, δ −0.71, −0.29, −0.09; **3c**$^+$, δ −0.69, −0.33, −0.09; **3d**$^+$, δ −0.70, −0.25, −0.06; **3b′**$^+$, δ −1.00, −0.79, −0.17; **3c′**$^+$, δ −0.97, −0.78, −0.19; **3d′**$^+$, δ −0.87, −0.77, −0.16.

(19) Qian, B.; Ward, D. L.; Smith, M. R., III. *Organometallics* **1998**, *17*, 3070.

similar trend, with the **4b**−**d**$^+$ resonances appearing at lower field than those of **2b**−**d**. In addition, the presence of only one N*Me*$_2$ resonance and one PhC*H*$_2$ resonance for **4b**−**d**$^+$ in CD_2Cl_2 at room temperature indicates an effective C_s symmetry, which is most likely due to a fast face exchange of THF on the NMR time scale.

The obtainment of cations **4b**−**d**$^+$ from the reaction of **3b**−**d**$^+$ with THF is consistent with the proposed adduct structure of these cations and shows that **3b**−**d**$^+$ can be considered as a formal source of three-coordinate {2-(CH_2L)-6-^{t}Bu-C_6H_3O}AlMe$^+$ cations stabilized by the corresponding neutral precursors {2-(CH_2L)-6-^{t}Bu-C_6H_3O}AlMe$_2$ acting as Lewis bases. In contrast, the outcome of the reaction of **3a**$^+$ with THF remains perplexing to us, given the apparent structural similarities in the solid state and in solution of all the obtained cations.

Reactivity of 3a$^+$ and 3b−d$^+$/3b′−d′$^+$ with Ethylene and Propylene Oxide (PO). Cations **3a**$^+$ and **3b**−**d**$^+$/**3b**′−**d**′$^+$ are not active in ethylene polymerization at 70 °C in toluene under 5 bar of ethylene pressure, as might be expected by the robustness and the lack of fluxional behavior of these adduct cations. These species do, however, initiate the polymerization of propylene oxide under mild conditions (room temperature, 15 min, toluene) to yield atactic PPO, as determined by ^{13}C NMR data (200 equiv of PO; conversion: **3b**$^+$/**3b**′$^+$, 55%; **3c**$^+$/**3c**′$^+$, 51%; **3d**$^+$/**3d**′$^+$, 61%). In contrast, **3a**$^+$ does not polymerize PO, which further illustrates the clear difference in reactivity of **3a**$^+$ vs **3b**−**d**$^+$/**3b**′−**d**′$^+$ toward Lewis bases. As estimated from SEC data, similar low-molecular-weight polymers are obtained with all three active cations (**3b**$^+$/**3b**′$^+$, $M_n = 2840$, $M_w/M_n = 1.54$; **3c**$^+$/**3c**′$^+$, $M_n = 2560$, $M_w/M_n = 1.61$; **3d**$^+$/**3d**′$^+$, $M_n = 3076$, $M_w/M_n = 1.50$). The polymerization activity of **3b**$^+$/**3b**′$^+$ was also tested at 0 °C (1 h, toluene), showing a higher conversion to PPO (70% conversion, $M_n = 9022$, $M_w/M_n = 1.73$). In this case, the obtained polymer possesses a much higher molecular weight, comparable to those of PPOs obtained with porphyrinato−aluminum chloride complexes.[20] The catalytic activity of **3b**−**d**$^+$/**3b**′−**d**′$^+$ at room temperature for PO polymerization compares with that of Schiff base−AlEt$_2$Cl initiator systems but is lower than that of porphyrinato−aluminum chloride complexes.[20,21]

Conclusions

This work shows that the mono(aminophenolate) Al dimethyl complexes **2a**−**d** can be cleanly converted to robust and stable dinuclear cationic Al alkyls (**3a**$^+$, **3b**−**d**$^+$/**3b**′−**d**′$^+$). Solid-state and solution studies as well as their reactivity with THF are consistent with **3b**−**d**$^+$/**3b**′−**d**′$^+$ being formal adducts of three-coordinate {2-(CH_2L)-6-^{t}Bu-C_6H_3O}AlMe$^+$ and the corresponding neutral precursors **2a**−**d** via an Al−μ_2-O−Al phenoxide bridge. In the case of **3a**$^+$, its apparent structural similarities with **3b**−**d**$^+$/**3b**′−**d**′$^+$ are in contrast with its difference of reactivity with Lewis bases such as THF and PO. In the present case, the higher stability of the obtained cations versus those derived from mono-(iminophenolate) Al dimethyl complexes may be related to the excellent flexibility of the chelating aminophenolate backbone, as illustrated by the molecular structures of **3a**$^+$ and **3b**′$^+$, allowing this ligand to adapt to the steric and electronic requirements of the chelated metal center. On the other hand, this good stability associated with the robustness of **3a**$^+$ and **3b**−**d**$^+$/**3b**′−**d**′$^+$ probably explains their lack of reactivity with ethylene.

Further studies will focus on a better understanding of the reactivity of **3a**$^+$ and on the design of new O,N bidentate ligands for the synthesis of more reactive cationic Al alkyls.

Chart 3

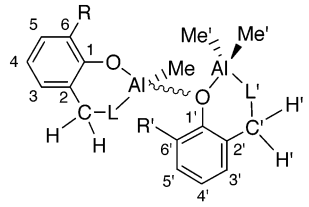

Experimental Section

General Procedures. All experiments were carried out under N_2 using standard Schlenk techniques or in a Mbraun Unilab glovebox. Benzene, pentane, and THF were distilled from Na/benzophenone and stored over activated molecular sieves (4 Å) in a glovebox prior to use. CH_2Cl_2 and CD_2Cl_2, were distilled from CaH_2 and stored over activated molecular sieves (4 Å) in a glovebox prior to use. C_6D_6 and C_6D_5Br were degassed under a N_2 flow and stored over activated molecular sieves (4 Å) in a glovebox prior to use. The aminophenols **1a**−**d** were synthesized according to general literature procedures, and NMR data for **1a**,**b** matched those in the literature.[22] $B(C_6F_5)_3$ was purchased from Strem Chemicals and was extracted with dry pentane prior to use. CD_2Cl_2, C_6D_6, and C_6D_5Br were purchased from Eurisotope. All other chemicals were purchased from Aldrich and were used as received. All NMR spectra were obtained on a Bruker AC 200 or 400 MHz spectrometer, in Teflon-valved J. Young tubes at ambient temperature, unless otherwise indicated. ^{1}H and ^{13}C chemical shifts are reported versus $SiMe_4$ and were determined by reference to the residual ^{1}H and ^{13}C solvent peaks. ^{11}B and ^{19}F chemical shifts are reported respectively versus $BF_3{\cdot}Et_2O$ in CD_2Cl_2 and versus neat $CFCl_3$. NMR assignments were supported by two-dimensional experiments (HMQC and HMBC) where appropriate. Size exclusion chromatography (SEC) analyses were carried out using a Waters 150CV instrument (M590 pump, U6K injector) equipped with a R410 refractometer and a Waters capillary viscometer and five Ultrastyragel columns (Waters). The SEC columns were eluted with THF at 40 °C at 1 mL/min. All the results are given in real molecular weight averages due to a universal calibration procedure. Elemental analyses were all performed by Mikroanalytisches Labor Pascher, Remagen-Bandorf, Germany, except those for **1c**−**e**, performed by the microanalysis laboratory of the Université Pierre et Marie Curie, Paris, France.

For the cationic Al species **3a**−**d**$^+$/**3a**′−**d**′$^+$, NMR assignments are quoted with reference to the general labeling chart given in Chart 3.

The cationic Al complexes were all obtained as fully dissociated MeB$(C_6F_5)_3^-$ salts in solution. The NMR data for the MeB$(C_6F_5)_3^-$ anion are listed below for all of the compounds.

(20) Sugimoto, H.; Kawamura, C.; Kuroki, M.; Aida, T.; Inoue, S. *Macromolecules* **1994**, *27*, 2013.

(21) Vincens, V.; Le Borgne, A.; Spassky, N. *Makromol. Chem. Rapid. Commun.* **1989**, *10*, 623.

(22) (a) Pochini, A.; Puglia, G.; Ungaro, R. *Synthesis* **1983**, *11*, 906. (b) Salakhutdinov, N. F.; Krysin, A. P.; Koptyug, V. A. *J. Org. Chem. USSR (Engl. Transl.)* **1990**, *26*, 664.

Data for MeB(C_6F_5)$_3^-$. ^{1}H NMR (400 MHz, CD_2Cl_2): δ 0.48 (B*Me*). ^{11}B{^{1}H} NMR (128 MHz, CD_2Cl_2): δ −11.9 (br s, *B*Me). ^{13}C{^{1}H} NMR (100 MHz, CD_2Cl_2): δ 148.6 (d, $^1J_{CF}$ = 233 Hz, *o*-C_6F_5), 137.9 (d, $^1J_{CF}$ = 238, *p*-C_6F_5), 136.7 (d, $^1J_{CF}$ = 233 Hz, *m*-C_6F_5), 10.3 (*Me*B). ^{19}F NMR (376 MHz, CD_2Cl_2): δ −133.5 (d, $^3J_{FF}$ = 19 Hz, 2F, *o*-C_6F_5), −165.7 (t, $^3J_{FF}$ = 20 Hz, 1F, *p*-C_6F_5), −168.2 (m, $^3J_{FF}$ = 19 Hz, 2F, *p*-C_6F_5).

2-($CH_2NC_4H_8$)-6-^{t}Bu-C_6H_3OH (1c) and 2-($CH_2NC_5H_{10}$)-6-^{t}Bu-C_6H_3OH (1d). In a 100 mL round-bottom flask, 2-^{t}Bu-C_6H_4OH (3.00 g, 20.0 mmol), formaldehyde (1.5 equiv, 2 mL of a 37% weight in water), and 1.3 equiv of the appropriate cyclic amine were added and dissolved in 50 mL of EtOH. The mixture was refluxed, and the reaction was monitored by TLC, revealing that the reaction was complete after 3 h. The mixture was then warmed to room temperature, and the volatiles were removed under vacuum. Pure **1c**,**d** were obtained after purification via a silica gel column chromatography using as an eluent system a 4/1 pentane/Et_2O mixture for **1c** (R_f = 0.25, 65% yield) and a 98/2 pentane/ethyl acetate mixture for **1d** (R_f = 0.20, 70% yield).

Data for 1c. ^{1}H NMR (200 MHz, $CDCl_3$): δ 1.52 (s, 9H, ^{t}Bu), 1.91 (m, 4H, H(β)−N), 2.70 (m, 4H, H(α)−N), 3.89 (s, 2H, PhC*H*$_2$), 6.79 (t, $^3J_{H,H}$ = 7.5 Hz, 1H, H(4)−PhO), 6.94 (dd, $^3J_{H,H}$ = 7.4 Hz, $^3J_{H,H}$ = 1.0 Hz, H(3)−PhO), 7.28 (dd, $^3J_{H,H}$ = 7.4 Hz, $^3J_{H,H}$ = 1.0 Hz, H(5)−PhO). ^{13}C{^{1}H} NMR (50 MHz, $CDCl_3$): δ 23.5 (C(β)−N), 29.2 (C*Me*$_3$), 34.4 (*C*Me$_3$), 53.0 (C(α)−N), 59.0 (Ph*C*H$_2$), 117.7 (C(4)−PhO), 122.5 (C(2)−PhO), 125.4 (C(3)− or C(5)−PhO), 125.7 (C(3)− or C(5)−PhO), 136.0 (C(6)−PhO), 156.8 (C(1)−PhO). Anal. Calcd for $C_{15}H_{23}NO$: C, 77.21; H, 9.93. Found: C, 77.17; H, 9.83.

Data for 1d. ^{1}H NMR (200 MHz, $CDCl_3$): δ 1.52 (s, 9H, ^{t}Bu), 1.58 (broad s, 2H, H(γ)−N), 1.72 (m, 4H, H(β)−N), 2.57 (broad s, 4H, H(α)−N), 3.73 (s, 2H, PhC*H*$_2$), 6.79 (t, $^3J_{H,H}$ = 7.5 Hz, 1H, H(4)−PhO), 6.92 (dd, $^3J_{H,H}$ = 7.5 Hz, $^3J_{H,H}$ = 1.0 Hz, H(3)−PhO), 7.26 (dd, $^3J_{H,H}$ = 7.4 Hz, $^3J_{H,H}$ = 1.0 Hz, H(5)−PhO). ^{13}C{^{1}H} NMR (50 MHz, $CDCl_3$): δ 24.0 (C(γ)−N), 25.7 (C(β)−N), 29.4 (C*Me*$_3$), 34.6 (*C*Me$_3$), 53.5 (C(α)−N), 62.4 (Ph*C*H$_2$), 118.0 (C(4)−PhO), 121.8 (C(2)−PhO), 125.6 (C(3) or C(5)−PhO), 126.6 (C(3) or C(5)−PhO), 136.3 (C(6)−PhO), 157.1 (C(1)−PhO). Anal. Calcd for $C_{16}H_{25}NO$: C, 77.68; H, 10.19. Found: C, 77.57; H, 10.02.

{2-(CH_2NMe_2)-6-R-C_6H_3O}$AlMe_2$ (2a, R = Ph; 2b, R = ^{t}Bu), {2-($CH_2NC_4H_8$)-6-^{t}Bu-C_6H_3O}$AlMe_2$ (2c), and {2-($CH_2NC_5H_{10}$)-6-^{t}Bu-C_6H_3O}$AlMe_2$ (2d). In a glovebox, a pentane solution (5 mL) of the appropriate aminophenol ligand **1a**−**d** (4.40 mmol) precooled to − 40 °C was slowly added via a pipet to a 20 mL vial containing a pentane solution (5 mL) of $AlMe_3$ (317 mg, 4.40 mmol), also precooled to − 40 °C. With a loosely capped vial to allow methane escape, the reaction mixture was warmed to room temperature and stirred for 2 h. The obtained white suspension was then evaporated to yield a colorless solid as a crude product. Recrystallization of this solid from a 10/1 pentane/Et_2O mixture at −40 °C afforded in all cases pure aluminum dimethyl complexes **2a**−**d** as colorless solids (**2a**, 87% yield; **2b**, 75% yield; **2c**, 70% yield; **2d**, 81% yield).

Data for 2a. ^{1}H NMR (400 MHz, C_6D_6): δ −0.59 (s, 6H, Al*Me*$_2$), 1.56 (s, 6H, N*Me*$_2$), 3.03 (s, 2H, PhC*H*$_2$), 6.64 (dd, $^3J_{H,H}$ = 7.0 Hz, $^4J_{H,H}$ = 1.7 Hz, 1H, H(3)−PhO), 6.79 (t, $^3J_{H,H}$ = 7.0 Hz, 1H, H(4)−PhO), 7.15 (t, $^3J_{H,H}$ = 8.0 Hz, 1H, H(4)−Ph), 7.31(t, $^3J_{H,H}$ = 7.9 Hz, 2H, H(2)− and H(6)−Ph), 7.47 (dd, $^3J_{H,H}$ = 7.2 Hz, $^3J_{H,H}$ = 1.6 Hz, 1H, H(5)−PhO), 7.91 (dd, $^3J_{H,H}$ = 8 Hz, $^4J_{H,H}$ = 2 Hz, 2H, H(3)− and H(5)−Ph). ^{13}C{^{1}H} NMR (100 MHz, C_6D_6): δ −11.2 (Al*Me*$_2$), 44.5 (N*Me*$_2$), 62.5 (Ph*C*H$_2$), 117.5 (C(4)−PhO), 121.8 (C(2)−PhO), 126.7 (C(6)−PhO), 129.0 (C(3)−PhO), 129.9 (C(4)− and C(6)−Ph), 131.9 (C(5)−PhO), 132.0 (C(3)− and C(5)−Ph), 140.2 (C(1)−Ph), 157.4 (C(1)−PhO). Anal. Calcd for $C_{17}H_{12}AlNO$: C, 72.06; H, 7.83. Found: C, 71.83;H, 8.09.

Data for 2b. ^{1}H NMR (400 MHz, C_6D_6): δ −0.50 (s, 6H, Al*Me*$_2$), 1.54 (s, 6H, N*Me*$_2$), 1.65 (s, 9H, ^{t}Bu), 3.02 (s, 2H, PhC*H*$_2$), 6.61 (dd, $^3J_{H,H}$ = 7.4 Hz, $^4J_{H,H}$ = 1.6, 1H, H(3)−PhO), 6.77 (t, $^3J_{H,H}$ = 7.4 Hz, 1H, H(4)−PhO), 7.40 (dd, $^3J_{H,H}$ = 7.8 Hz, $^4J_{H,H}$ = 1.8 Hz, 1H, H(5)−PhO). ^{13}C{^{1}H} NMR (100 MHz, C_6D_6): δ −10.9 (Al*Me*$_2$), 30.1 (C*Me*$_3$), 35.3 (*C*Me$_3$), 44.6 (N*Me*$_2$), 62.7 (Ph*C*H$_2$), 117.5 (C(4)−PhO), 122.1 (C(2)−PhO), 128.4 (C(3)−PhO), 129.2 (C(5)−PhO), 139.5 (C(6)−PhO), 158.4 (C(1)−PhO). ^{1}H NMR (400 MHz, CD_2Cl_2, 25 °C): δ −0.76 (s, 6H, Al*Me*$_2$), 1.41 (s, 9H, ^{t}Bu), 2.41 (s, 6H, N*Me*$_2$), 3.75 (s, 2H, PhC*H*$_2$), 6.63 (t, $^3J_{H,H}$ = 7.4 Hz, 1H, H(4)−PhO), 6.86 (dd, $^3J_{H,H}$ = 7.4 Hz, $^4J_{H,H}$ = 1.6 Hz, 1H, H(3)−PhO), 7.23 (dd, $^3J_{H,H}$ = 7.8 Hz, $^4J_{H,H}$ = 1.8 Hz, 1H, H(5)−PhO). Anal. Calcd for $C_{15}H_{26}AlNO$: C, 68.41; H, 9.95. Found: C, 68.31; H, 10.19.

Data for 2c. ^{1}H NMR (400 MHz, CD_2Cl_2): δ −0.77 (Al*Me*$_2$), 1.40 (s, 9H, ^{t}Bu), 1.90−2.05 (m, 4H, H(β)−N), 2.63 (m, 2H, H(α)−N), 3.12 (m, 2H, H(α)−N), 3.82 (s, 2H, PhC*H*$_2$), 6.61 (t, $^3J_{H,H}$ = 7.4 Hz, 1H, H(4)−PhO), 6.87 (dd, $^3J_{H,H}$ = 7.5 Hz, $^4J_{H,H}$ = 1.8 Hz, 1H, H(3)−PhO), 7.23 (dd, $^3J_{H,H}$ = 7.5 Hz, $^4J_{H,H}$ = 1.8 Hz, 1H, H(5)−PhO). ^{13}C{^{1}H} NMR (400 MHz, CD_2Cl_2): δ −11.9 (Al*Me*$_2$), 22.2 (C(β)−N), 28.9 (C*Me*$_3$), 34.3 (*C*Me$_3$), 54.1 (C(α)−N), 59.1 (Ph*C*H$_2$), 115.9 (C(4)−PhO), 122.2 (C(2)−PhO), 126.9 (C(3)−PhO), 127.3 (C(5)−PhO), 138.4 (C(6)−PhO), 158.6 (C(1)−PhO). Anal. Calcd for $C_{17}H_{28}AlNO$: C, 70.56; H, 9.75. Found: C, 70.44; H, 9.86.

Data for 2d. ^{1}H NMR (400 MHz, CD_2Cl_2): δ −0.72 (Al*Me*$_2$), 1.40 (s, 9H, ^{t}Bu), 1.55 (m, 1H, H(γ)−N), 1.69 (m, 5H, H(γ)− and H(β)−N), 2.44 (m, 2H, H(α)−N), 3.09 (m, 2H, H(α)−N), 3.83 (s, 2H, PhC*H*$_2$), 6.62 (t, $^3J_{H,H}$ = 7.5 Hz, 1H, H(4)−PhO), 6.90 (dd, $^3J_{H,H}$ = 7.5 Hz, $^4J_{H,H}$ = 1.8 Hz, 1H, H(3)−PhO), 7.23 (dd, $^3J_{H,H}$ = 7.5 Hz, $^4J_{H,H}$ = 1.8 Hz, 1H, H(5)−PhO). ^{13}C{^{1}H} NMR (400 MHz, CD_2Cl_2): δ −10.6 (Al*Me*$_2$), 20.9 (C(β)−N), 22.7 (C(γ)−N), 28.7 (C*Me*$_3$), 34.1 (*C*Me$_3$), 53.2 (C(α)−N), 59.0 (Ph*C*H$_2$), 116.0 (C(4)−PhO), 120.8 (C(2)−PhO), 126.9 (C(3)−PhO), 126.8 (C(5)−PhO), 138.0 (C(6)−PhO), 158.5 (C(1)−PhO). Anal. Calcd for $C_{18}H_{30}AlNO$: C, 71.25; H, 9.97. Found: C, 71.14; H, 10.10.

[{2-(CH_2NMe_2)-6-Ph-C_6H_3O}$_2Al_2Me_3$][MeB(C_6F_5)$_3$] ([3a][MeB(C_6F_5)$_3$]). In a glovebox, equimolar amounts of {6-(CH_2NMe_2)-2-Ph-C_6H_3O}$AlMe_2$ (**2a**) (90.0 mg, 0.318 mmol) and B(C_6F_5)$_3$ (81.6 mg, 0.159 mmol) were added to a sample vial and dissolved in 1 mL of CH_2Cl_2. The resulting colorless solution was stirred for 1 h at room temperature and then evaporated to dryness to yield a colorless foam. Trituration with cold pentane provoked the precipitation of a colorless solid. The mixture was filtered through a glass frit and the solid residue dried under vacuum to afford pure [**3a**][MeB(C_6F_5)$_3$] as a colorless solid (131 mg, 76% yield). Complete assignments of the ^{1}H and ^{13}C NMR resonances of **3a**$^+$ were possible using a combination of HMQC and HMBC 2D NMR techniques, and these data are listed below.

Data for 3a$^+$. ^{1}H NMR (400 MHz, CD_2Cl_2, 35 °C):[23] δ −1.06 (s, 3H, Al*Me*), −0.89 (s, 3H, Al*Me*′), −0.83 (s, 3H, Al*Me*′), 1.43 (s, 3H, N*Me*′), 1.58 (s, 3H, N*Me*′), 2.18 (s, 3H, N*Me*), 2.21 (s, 3H, N*Me*), 3.21 (d, $^2J_{HH}$ = 13 Hz, 1H, PhC*H*$_2$), 3.44 (d, $^2J_{HH}$ = 14 Hz, 1H, PhC*H*′$_2$), 4.05 (d, $^2J_{HH}$ = 13 Hz, 1H, PhC*H*$_2$), 4.10 (d, $^2J_{HH}$ = 14.1 Hz, 1H, PhC*H*′$_2$), 6.92 (t, $^3J_{HH}$ = 8.1 Hz, 1H, H(4)−PhO), 7.00 (dd, $^2J_{HH}$ = 7.9 Hz, $^2J_{HH}$ = 2 Hz, 1H, H(3)−PhO), 7.31−7.36 (m, 3H, H′(3)−PhO and H(2)− and H(6)−Ph), 7.39−7.44 (m, 3H, H′(4)−PhO and H′(2)− and H′(6)−Ph), 7.48−7.57 (m, 8H, Ph and PhO). ^{13}C{^{1}H} NMR (100 MHz, CD_2Cl_2): δ −10.6 (Al*Me*), −10.3 (Al*Me*′), −9.8 (Al*Me*′), 43.0 (N*Me*′), 45.4 (N*Me*), 46.5 (N*Me*′), 46.7 (N*Me*), 60.8 (Ph*C*′H$_2$), 63.4 (Ph*C*H$_2$), 119.3 (C(2)−PhO), 120.0 (C(4)−PhO), 125.7 (C′(2)−PhO), 127.1 (C(2)− and C(6)−Ph), 127.5 (C′(4)−PhO), 128.2 (C′(2)− and C′(6)−Ph), 129.2 (C(6)−PhO), 129.4 (C(3)− and C(5)−Ph), 129 5 (C′(3)− and C′(5)−Ph), 129.6

(23) The ^{1}H NMR spectrum of **3a**$^+$ at room temperature is almost identical with that at 35 °C, except that it contains two Al*Me* signals in a 2/1 ratio versus three AlMe resonances in a 1/1/1 ratio at 35 °C, as expected for the C_1-symmetric **3a**$^+$. We assumed that two Al*Me* resonances for **3a**$^+$ have coincidentally the same chemical shift at room temperature.

(C′(4)−Ph), 131.2 (C(3)−PhO), 131.3 (C(5)−PhO), 132.4 (C′(3)−PhO), 134.8 (C′(5)−PhO), 135.5 (C′(6)−PhO), 137.2 (C(1)−Ph), 138.6 (C′(1)−Ph), 146.9 (C′(1)−PhO), 153.4 (C(1)−PhO). Anal. Calcd for $C_{52}H_{44}Al_2BF_{15}N_2O_2$: C, 57.89; H, 4.12. Found: C, 57.51;H, 4.02.

[{2-(CH_2NMe_2)-6-^{t}Bu-C_6H_3O}$_2$$Al_2Me_3$][$MeB(C_6F_5)_3$] ([3b/3b′][$MeB(C_6F_5)_3$]). In a glovebox, {6-($CH_2NMe_2$)-2-^{t}Bu-$C_6H_3O$}-$AlMe_2$ (**2b**; 150.0 mg, 0.570 mmol) and $B(C_6F_5)_3$ (81.6 mg, 0.285 mmol) were added to a sample vial and dissolved in 1 mL of CH_2Cl_2. The resulting colorless solution was stirred for 15 min at room temperature and was evaporated to dryness to yield a colorless foam. Trituration with cold pentane followed by filtration through a glass frit of the precipitated solid afforded, after drying under vacuum, a pure 1/1 mixture of [**3b**][MeB-$(C_6F_5)_3$] and [**3b′**][$MeB(C_6F_5)_3$] as a colorless solid (190 mg, 81% yield). Anal. Calcd for $C_{48}H_{52}Al_2BF_{15}N_2O_2$: C, 55.50; H, 4.82. Found: C, 55.77; H, 5.07. Complete assignments of the ^{1}H and ^{13}C NMR resonances of **3b**$^+$ and **3b′**$^+$ were possible using a combination of HMQC and HMBC 2D NMR techniques, and these data are listed below.

Data for 3b$^+$. ^{1}H NMR (400 MHz, CD_2Cl_2): δ −0.71 (s, 3H, Al*Me*′), −0.29 (s, 3H, Al*Me*), −0.09 (s, 3H, Al*Me*′), 1.45 (s, 9H, ^{t}Bu), 1.52 (s, 9H, ^{t}Bu′), 2.18 (s, 3H, N*Me*), 2.19 (s, 3H, N*Me*′), 2.30 (s, 3H, N*Me*), 2.76 (s, 3H, N*Me*′), 3.05 (d, $^2J_{HH}$ = 14 Hz, 1H, PhCH_2), 3.28 (d, $^2J_{HH}$ =14 Hz, 1H, PhCH'_2), 3.64 (d, $^2J_{HH}$ = 14, 1H, PhCH_2), 4.84 (d, $^2J_{HH}$ = 14 Hz, 1H, PhCH'_2), 6.82 (broad d, 2H, H(3)− and H(4)−PhO), 7.21 (dd, $^3J_{HH}$ = 8 Hz, $^4J_{HH}$ = 2, H′(3)−PhO), 7.36−7.42 (m, 2H, H(5) and H′(4)−PhO), 7.76 (dd, $^3J_{HH}$ = 8 Hz, $^4J_{HH}$ = 2 Hz, 1H, H′(5)−Ph). ^{13}C{^{1}H} NMR (100 MHz, CD_2Cl_2): δ −12.1 (Al*Me*), −9.8 (Al*Me*′), −9.5 (Al*Me*′), 29.4 (C(*C*H_3)$_3$), 32.9 (C(*C*′H_3)$_3$), 34.4 (*C*(CH_3)$_3$), 36.6 (*C*′(CH_3)$_3$), 44.8 (N*Me*), 46.8 (N*Me*′), 47.3 (N*Me*), 48.1 (N*Me*′), 62.1 (PhC′H_2), 63.1 (Ph*C*H_2), 119.8 (C(4)−PhO), 120.3$_3$ (C(2)−PhO), 127.3 (C′(2)−PhO), 127.5 (C′(4)−PhO), 128.2 (C(3)−PhO), 129.2 (C(5)−PhO), 131.0 (C′(3)−PhO), 134.5 (C′(5)−PhO), 139.1 (C(6)−PhO), 142.4 (C′(6)−PhO), 146.0 (C′(1)−PhO), 154.0 (C(1)−PhO).

Data for 3b′$^+$. ^{1}H NMR (400 MHz, CD_2Cl_2): δ −1.00 (s, 3H, Al*Me*), −0.79 (s, 3H, Al*Me*′), −0.17 (s, 3H, Al*Me*′), 1.35 (s, 9H, ^{t}Bu), 1.51 (s, 9H, ^{t}Bu′), 2.33 (s, 3H, N*Me*′), 2.48 (s, 3H, N*Me*), 2.80 (s, 3H, N*Me*′), 2.97 (s, 3H, N*Me*), 3.34 (d, $^2J_{HH}$ = 14 Hz, 1H, PhCH_2), 3.42 (d, $^2J_{HH}$ = 14 Hz, 1H, PhCH'_2), 4.68 (d, $^2J_{HH}$ = 14 Hz, 1H, PhCH_2), 5.53 (d, $^2J_{HH}$ = 14 Hz, 1H, PhCH'_2), 6.90 (t, 1H, $^3J_{HH}$ = 8 Hz, H(4)−PhO), 7.04 (dd, 1H, $^3J_{HH}$ = 7 Hz, $^4J_{HH}$ = 2 Hz, H(3)−PhO), 7.28 (dd, $^3J_{HH}$ = 8 Hz, $^4J_{HH}$ = 2 Hz, 1H, H′(3)−PhO), 7.36−7.42 (m, 2H, H(5)− and H′(4)−PhO), 7.76 (dd, $^3J_{HH}$ = 8 Hz, $^4J_{HH}$ = 2 Hz, 1H, H′(5)−Ph). ^{13}C{^{1}H} NMR (100 MHz, CD_2Cl_2): δ −13.1 (Al*Me*), −10.2 (Al*Me*′), −7.7 (Al*Me*′), 29.2 (C(*C*H_3)$_3$), 33.0 (C(*C*′H_3)$_3$), 34.2 (*C*(CH_3)$_3$), 36.5 (*C*′(CH_3)$_3$), 46.1 (N*Me*′), 46.9 (N*Me*), 48.2 (N*Me*), 48.4 (N*Me*′), 61.5 (PhC′H_2), 65.0 (Ph*C*H_2), 120.3$_2$ (C(4)−PhO), 121.6 (C(2)−PhO), 126.8 (C′(2)−PhO), 127.7 (C′(4)−PhO), 128.5 (C(3)−PhO), 128.9 (C(5)−PhO), 130.8 (C′(3)−PhO), 134.2 (C′(5)−PhO), 139.4 (C(6)−PhO), 141.9 (C′(6)−PhO), 146.9 (C′(1)−PhO), 154.7 (C(1)−PhO). Anal. Calcd for $C_{48}H_{52}Al_2BF_{15}N_2O_2$: C, 55.50; H, 4.82. Found: C, 54.77; H, 5.07.

[{2-($CH_2NC_4H_8$)-6-^{t}Bu-C_6H_3O}$_2$$Al_2Me_3$][$MeB(C_6F_5)_3$] ([3c/3c′][$MeB(C_6F_5)_3$]) and [{2-($CH_2NC_5H_{10}$)-6-^{t}Bu-$C_6H_3O$}$_2$-$Al_2Me_3$][$MeB(C_6F_5)_3$] ([3d/3d′][$MeB(C_6F_5)_3$]). Compounds [**3c/3c′**][$MeB(C_6F_5)_3$] and [**3d/3d′**][$MeB(C_6F_5)_3$] were obtained by following the same procedure and using the same quantities as those for [**3b/3b′**][$MeB(C_6F_5)_3$] and were obtained in a 3/1 ratio, respectively, in 81% and 75% overall yields. Complete assignments of the ^{1}H and ^{13}C NMR resonances of **3c**$^+$/**3c′**$^+$ and **3d**$^+$/**3d′**$^+$ were also possible using a combination of HMQC and HMBC 2D-NMR techniques, and these data are listed below.

Data for 3c$^+$ (Major Isomer, 75%). ^{1}H NMR (400 MHz, CD_2Cl_2): δ −0.69 (s, 3H, Al*Me*′), −0.33 (s, 3H, Al*Me*), −0.09 (s, 3H, Al*Me*′), 1.47 (s, 9H, ^{t}Bu), 1.51 (s, 9H, ^{t}Bu′), 1.70−2.20 (m, 8H, H(β)−N and H′(β)−N), 2.45 (m, 1H, H′(α)−N), 2.55−3.20 (m, 6H, H(α)−N and H′(α)−N), 3.12 (d, $^2J_{HH}$ = 14 Hz, 1H, PhCH_2), 3.34 (d, $^2J_{HH}$ = 14 Hz, 1H, PhCH'_2), 3.41 (d, $^2J_{HH}$ = 14, 1H, PhCH_2), 3.50 (m, 1H, H(α)−N), 4.93 (d, $^2J_{HH}$ = 14 Hz, 1H, PhCH'_2), 6.78 (broad d, 2H, H(3) and H(4)−PhO), 7.16 (dd, $^3J_{HH}$ = 8 Hz, $^4J_{HH}$ = 2, H′(3)−PhO), 7.34 (m, 1H, H′(4)−PhO), 7.39 (m, 2H, H′(3)− and H(5)−PhO), 7.74 (dd, $^3J_{HH}$ = 8 Hz, $^4J_{HH}$ = 2 Hz, 1H, H′(5)−Ph). ^{13}C{^{1}H} NMR (100 MHz, CD_2Cl_2): δ −11.5 (Al*Me*), −9.7$_2$ (Al*Me*′), −9.7$_1$ (Al*Me*′), 20.2 (C(β)−N), 21.0 (C(β)−N), 21.1 (C′(β)−N), 22.0 (C′(β)−N), 29.3 (C(*C*H_3)$_3$), 32.9 (C(*C*′H_3)$_3$), 34.4 (*C*(CH_3)$_3$), 36.6 (*C*′(CH_3)$_3$), 52.0 (C(α)−N), 55.0 (C′(α)−N), 55.8 (C′(α)−N), 56.8 (C(β)−N), 57.2 (PhC′H_2), 58.1 (Ph*C*H_2), 119.5 (C(4)−PhO), 120.7 (C(2)−PhO), 127.5 (C′(2)−PhO), 128.1 (C′(4)−PhO), 128.3 (C(3)−PhO), 128.7 (C(5)−PhO), 130.2 (C′(3)−PhO), 134.2 (C′(5)−PhO), 139.5 (C(6)−PhO), 142.3 (C′(6)−PhO), 146.1 (C′(1)−PhO), 154.2 (C(1)−PhO).

Data for 3c′$^+$ (Minor Isomer, 25%). ^{1}H NMR (400 MHz, CD_2Cl_2): δ −0.97 (s, 3H, Al*Me*), −0.78 (s, 3H, Al*Me*′), −0.19 (s, 3H, Al*Me*′), 1.38 (s, 9H, ^{t}Bu), 1.47 (s, 9H, ^{t}Bu′), 1.70−2.20 (m, 7H, H(β)−N and H′(β)−N), 2.25 (m, 1H, H′(β)−N), 2.55−3.20 (m, 6H, H(α)−N and H′(α)−N), 3.45−3.55 (m, 4H, 2H(α)−N and 1PhCH_2), 3.56 (d, $^2J_{HH}$ = 14 Hz, 1H, 1PhCH'_2), 4.36 (d, $^2J_{HH}$ = 14 Hz, 1H, PhCH_2), 5.53 (d, $^2J_{HH}$ = 14 Hz, 1H, PhCH'_2), 6.77 (m, 1H, H(4)−PhO), 6.84 (dd, $^3J_{HH}$ = 8 Hz, $^4J_{HH}$ = 2 Hz, 1H, H(3)−PhO), 6.98 (dd, $^3J_{HH}$ = 8 Hz, $^4J_{HH}$ = 2 Hz, 1H, H′(3)−PhO), 7.24 (dd, 1H, $^3J_{HH}$ = 8 Hz, $^4J_{HH}$ = 2 Hz, H(5)−PhO), 7.39 (m, 1H, H′(4)−PhO), 7.68 (dd, $^3J_{HH}$ = 8 Hz, $^4J_{HH}$ = 2 Hz, 1H, H′(5)−Ph). ^{13}C{^{1}H} NMR (100 MHz, CD_2Cl_2): δ −12.1 (Al*Me*), −10.4 (Al*Me*′), −8.6 (Al*Me*′), 20.9 (C(β)−N), 21.1 (C(β)−N), 21.8 (C′(β)−N), 22.6 (C′(β)−N), 29.0 (C(*C*H_3)$_3$), 32.9$_3$ (C(*C*′H_3)$_3$), 34.2 (*C*(CH_3)$_3$), 36.5 (*C*′(CH_3)$_3$), 54.6 (C(α)−N), 55.7 (C′(α)−N), 56.2 (C′(α)−N), 57.4 (C(β)−N), 57.9 (PhC′H_2), 59.6 (Ph*C*H_2), 119.9 (C(4)−PhO), 121.9 (C(2)−PhO), 126.9 (C′(2)−PhO), 127.6 (C′(4)−PhO), 128.3 (C(3)−PhO), 129.0 (C(5)−PhO), 130.0 (C′(3)−PhO), 134.1 (C′(5)−PhO), 139.4 (C(6)−PhO), 141.7 (C′(6)−PhO), 146.7 (C′(1)−PhO), 155.3 (C(1)−PhO).

Data for 3d$^+$ (Major Isomer, 75%). ^{1}H NMR (400 MHz, CD_2Cl_2): δ −0.70 (s, 3H, Al*Me*′), −0.25 (s, 3H, Al*Me*), −0.06 (s, 3H, Al*Me*′), 1.22−1.96 (m, 12H, H(β)−N, H′(β)−N, H(γ)−N, and H′(γ)−N), 1.44 (s, 9H, ^{t}Bu), 1.50 (s, 9H, ^{t}Bu′), 2.15−2.33 (m, 2H, H(α)−N), 2.45 (broad d, 1H, H′(α)−N), 2.61−2.77 (m, 3H, H(α)−N and H′(α)−N), 3.12 (dt, 1H, $^2J_{HH}$ = 13 Hz, J_{HH} = 4 Hz, H′(α)−N), 3.28 (d, $^2J_{HH}$ = 14 Hz, 1H, PhCH_2), 3.44 (d, $^2J_{HH}$ = 14 Hz, 1H, PhCH'_2), 3.56 (broad m, 1H, $^2J_{HH}$ = 13 Hz, H′(α)−N), 3.92 (d, $^2J_{HH}$ = 14 Hz, 1H, PhCH_2), 4.61 (d, $^2J_{HH}$ = 14 Hz, 1H, PhCH'_2), 6.82 (t, 1H, $^3J_{HH}$ = 8 Hz, H(4)−PhO), 6.88 (m, 1H, H(3)−PhO), 7.17 (dd, $^3J_{HH}$ = 8 Hz, $^4J_{HH}$ = 2 Hz, H′(3)−PhO), 7.32 (t, 1H, $^3J_{HH}$ = 8 Hz, H′(4)−PhO), 7.39 (dd, 1H, $^3J_{HH}$ = 8 Hz, $^4J_{HH}$ = 2 Hz, H(5)−PhO), 7.70 (dd, $^3J_{HH}$ = 8 Hz, $^4J_{HH}$ = 2 Hz, 1H, H′(5)−Ph). ^{13}C{^{1}H} NMR (100 MHz, CD_2Cl_2): δ −11.0 (Al*Me*), −8.7 (Al*Me*′), −8.5$_1$ (Al*Me*′), 16.7 (C(γ)−N), 16.9 (C′(γ)−N), 21.7 (C′(β)−N), 21.8 (C(β)−N), 21.9 (C′(β)−N), 22.1 (C(β)−N), 29.4 (C(*C*H_3)$_3$), 32.9 (C(*C*′H_3)$_3$), 34.4 (*C*(CH_3)$_3$), 36.5 (*C*′(CH_3)$_3$), 49.9 (C(α)−N), 51.6 (C′(α)−N), 51.7 (C′(α)−N), 53.0 (C(α)−N), 55.2 (PhC′H_2), 56.9 (Ph*C*H_2), 119.3 (C(2)−PhO), 119.7 (C(4)−PhO), 126.3 (C′(2)−PhO), 127.4 (C′(4)−PhO), 128.3 (C(3)−PhO), 128.9 (C(5)−PhO), 131.0 (C′(3)−PhO), 134.5 (C′(5)−PhO), 139.1 (C(6)−PhO), 142.1 (C′(6)−PhO), 146.5 (C′(1)−PhO), 154.7 (C(1)−PhO).

Data for 3d′$^+$ (Minor Isomer, 25%). ^{1}H NMR (400 MHz, CD_2Cl_2): δ −0.87 (s, 3H, Al*Me*), −0.77 (s, 3H, Al*Me*′), −0.16 (s, 3H, Al*Me*′), 1.22−1.96 (m, 12H, H(β)−N, H′(β)−N, H(γ)−N, and H′(γ)−N), 1.35 (s, 9H, ^{t}Bu), 1.37 (s, 9H, ^{t}Bu′), 2.07−2.48 (m, 3H, H(α)−N and H′(α)−N), 2.55−2.77 (m, 1H, H(α)−N), 2.80 (m, 1H, H′(α)−N), 2.90 (m, 1H, H(α)−N), 3.06 (m, 1H, H′(α)−N), 3.34 (m, 1H, H′(α)−N), 3.77 (d, $^2J_{HH}$ = 14 Hz, 1H, PhCH'_2), 4.21 (d, $^2J_{HH}$ = 14 Hz, 1H, PhCH_2), 4.33 (d, $^2J_{HH}$ = 14 Hz, 1H, PhCH_2), 5.30 (d, $^2J_{HH}$ = 14 Hz, 1H, PhCH'_2), 6.87 (t, 1H, $^3J_{HH}$ = 8 Hz, H(4)−PhO), 6.88 (m, 1H, H(3)−PhO),

7.05 (dd, $^3J_{HH}$ = 8 Hz, $^4J_{HH}$ = 2 Hz, 1H, H′(3)−PhO), 7.25 (dd, 1H, $^3J_{HH}$ = 8 Hz, $^4J_{HH}$ = 2 Hz, H(5)−PhO), 7.37 (m, 1H, H′(4)−PhO), 7.67 (dd, $^3J_{HH}$ = 8 Hz, $^4J_{HH}$ = 2 Hz, 1H, H′(5)−Ph). $^{13}C\{^1H\}$ NMR (100 MHz, CD_2Cl_2): δ −11.3 (Al*Me*), −9.0 (Al*Me*′), −8.2 (Al*Me*′), 17.0 (C(γ)−N), 17.6 (C′(γ)−N), 21.9 (C(β)−N), 22.1 (C(β)−N), 22.5 (C′(β)−N), 22.6 (C′(β)−N), 29.2 (C(*C*H_3)$_3$), 33.0 (C(*C*′H_3)$_3$), 34.2 (*C*(CH$_3$)$_3$), 36.6 (*C*′(CH$_3$)$_3$), 50.2 (C(α)−N), 52.2 (C′(α)−N), 52.5 (C′(α)−N), 53.2 (C(α)−N), 53.5 (Ph*C*′H$_2$), 59.6 (Ph*C*H$_2$), 120.0 (C(4)−PhO), 120.5 (C(2)−PhO), 126.3$_2$ (C′(2)−PhO), 127.2 (C′(4)−PhO), 128.4 (C(3)−PhO), 128.8 (C(5)−PhO), 130.8 (C′(3)−PhO), 134.2 (C′(5)−PhO), 139.3 (C(6)−PhO), 141.9 (C′(6)−PhO), 147.1 (C′(1)−PhO), 155.2 (C(1)−PhO).

Generation of [{2-(CH$_2$L)-6-^{t}Bu-C$_6$H$_3$O}Al(Me)(THF)][MeB(C$_6$F$_5$)$_3$] ([4b−d][MeB(C$_6$F$_5$)$_3$]: 4b$^+$, L = NMe$_2$; 4c$^+$, L = NC$_4$H$_8$; 4d$^+$, L = NC$_5$H$_{10}$). In a sample vial, [**3b**−**d**/**3b**′−**d**′][MeB(C$_6$F$_5$)$_3$] (0.08 mmol) were dissolved in 0.75 mL of CD_2Cl_2 and 1 equiv of THF (6.5 μL, 0.08 mmol) was added via a syringe at room temperature. The vial was vigorously shaken at room temperature, and a ^1H NMR spectrum was recorded after 10 min, showing the quantitative conversion of [**3b**−**d**/**3b**′−**d**′][MeB(C$_6$F$_5$)$_3$] to **2b**−**d** and [**4b**/**4d**][MeB(C$_6$F$_5$)$_3$]in a 1/1 ratio. The resulting mixture was also characterized by ^{13}C and ^{19}F NMR.

Data for 4b$^+$. ^1H NMR (200 MHz, CD_2Cl_2): δ −0.33 (Al*Me*), 0.50 (br, 3H, *Me*B), 1.41 (s, 9H, ^{t}Bu), 2.21 (m, 4H, H(β)−THF), 2.59 (s, 6H, N*Me*$_2$), 3.89 (s, 2H, PhCH_2), 4.33 (m, 4H, H(β)−THF), 6.88 (t, $^3J_{H,H}$ = 7.5 Hz, 1H, H(4)−PhO), 6.99 (dd, $^3J_{H,H}$ = 7.4 Hz, $^4J_{H,H}$ = 1.6, 1H, H(3)−PhO), 7.41 (dd, $^3J_{H,H}$ = 7.8 Hz, $^4J_{H,H}$ = 1.8 Hz, 1H, H(5)−PhO). $^{13}C\{^1H\}$ NMR (100 MHz, CD_2Cl_2, 25 °C): δ −17.7 (Al*Me*), 25.1 (H(β)−THF), 28.9 (C*Me*$_3$), 34.4 (*C*Me$_3$), 44.1 (N*Me*$_2$), 63.0 (PhCH_2), 74.1 (H(α)−THF), 119.3 (C(2)−PhO), 119.9 (C(4)−PhO), 128.0 (C(3)−PhO), 128.8 (C(5)−PhO), 139.3 (C(6)−PhO), 154.5 (C(1)−PhO).

Data for 4c$^+$. ^1H NMR (200 MHz, CD_2Cl_2): δ −0.37 (Al*Me*), 0.50 (br, 3H, *Me*B), 1.41 (s, 9H, ^{t}Bu), 1.80−2.10 (m, 2H, H(β)−N), 2.18 (m, 2H, H(β)−N), 2.29 (m, 4H, H(β)−THF), 3.03 (m, 4H, H(α)−N), 3.89 (s, 2H, PhCH_2), 4.46 (m, 4H, H(β)−THF), 6.85 (t, $^3J_{H,H}$ = 7.5 Hz, 1H, H(4)−PhO), 6.95 (dd, $^3J_{H,H}$ = 7.4 Hz, $^4J_{H,H}$ = 1.6, 1H, H(3)−PhO), 7.38 (dd, $^3J_{H,H}$ = 7.8 Hz, $^4J_{H,H}$ = 1.8 Hz, 1H, H(5)−PhO). $^{13}C\{^1H\}$ NMR (100 MHz, CD_2Cl_2, 25 °C): δ −17.4 (Al*Me*), 21.6 (C(β)−N), 25.1 (C(β)−THF), 28.9 (C*Me*$_3$), 34.4 (*C*Me$_3$), 53.4 (C(α)−N), 58.5 (Ph*C*H$_2$), 75.5 (C(α)−THF), 119.7 (C(4)−PhO), 120.0 (C(2)−PhO), 127.9 (C(3)−PhO), 128.7 (C(5)−PhO), 139.3 (C(6)−PhO), 154.8 (C(1)−PhO).

Data for 4d$^+$. ^1H NMR (200 MHz, CD_2Cl_2): δ −0.27 (Al*Me*), 0.50 (br, 3H, *Me*B), 1.40 (s, 9H, ^{t}Bu), 1.50−1.80 (m, 4H, H(β)− and H(γ)−N), 1.94 (br, 2H, H(β)−N), 2.30 (m, 4H, H(β)−THF), 2.73 (br, 2H, H(α)−N), 3.12 (br, 2H, H(α)−N), 4.01 (s, 2H, PhCH_2), 4.49 (m, 4H, H(α)−THF), 6.86 (t, $^3J_{H,H}$ = 7.5 Hz, 1H, H(4)−PhO), 7.00 (dd, $^3J_{H,H}$ = 7.4 Hz, $^4J_{H,H}$ = 1.6, 1H, H(3)−PhO), 7.38 (dd, $^3J_{H,H}$ = 7.8 Hz, $^4J_{H,H}$ = 1.8 Hz, 1H, H(5)−PhO). $^{13}C\{^1H\}$ NMR (100 MHz, CD_2Cl_2, 25 °C): δ −14.8 (Al*Me*), 19.8 (C(γ)−N), 21.8 (C(β)−THF), 25.1 (C(β)−THF), 29.0 (C*Me*$_3$), 34.4 (*C*Me$_3$), 53.3 (C(α)−N), 57.8 (Ph*C*H$_2$), 76.0 (C(α)−THF), 118.6 (C(2)−PhO), 119.8 (C(4)−PhO), 128.0 (C(3)−PhO), 128.7 (C(5)−PhO), 139.0 (C(6)−PhO), 154.8 (C(1)−PhO).

Generation of {2-(CH$_2$NMe$_2$)-6-^{t}Bu-4-Me-C$_6$H$_2$O}Al(Me)(C$_6$F$_5$) (5b) via Decomposition of (3b/3b′)(MeB(C$_6$F$_5$)$_3$). The salt compound [**3b**/**3b**′][MeB(C$_6$F$_5$)$_3$] (83.0 mg, 0.08 mmol) was charged in a J. Young tube, and 0.75 mL of C_6D_6 was added. The NMR tube was vigorously shaken to yield a two-phase mixture that was immersed in an oil bath at 75 °C. The reaction was monitored by ^1H NMR, which revealed the complete conversion of [**3b**/**3b**′][MeB(C$_6$F$_5$)$_3$] to a 1/1/1 mixture of **5b**, **2b**, and MeB(C$_6$F$_5$)$_2$ after 5 h at 75 °C in C_6D_6. The ^1H, ^{11}B, ^{13}C, and ^{19}F NMR data for MeB(C$_6$F$_5$)$_2$ matched those of the literature.[17]

Preparative-Scale Generation of 5b. The salt compound [**3b**/**3b**′][MeB(C$_6$F$_5$)$_3$] (231.6 mg, 0.285 mmol) was charged in a small Schlenk tube, and 10 mL of benzene was added to yield a two-phase mixture which was heated at 70 °C for 18 h. The volatiles were then removed under vacuum to afford crude **5b** as a yellowish powder. Recrystallization from pentane at −40 °C afforded pure **5b** as a colorless powder (40 mg, 34% yield). ^1H NMR (200 MHz, C_6D_6): δ −0.37 (t, $^5J_{HF}$ = 1.4 Hz, 3H, Al*Me*), 1.51 (s, 3H, N*Me*), 1.56 (s, 9H, C*Me*$_3$), 1.59 (s, 3H, N*Me*), 2.67 (d, $^2J_{HH}$ = 14 Hz, 1H, PhCH_2), 3.34 (d, $^2J_{HH}$ = 14 Hz, 1H, PhCH_2), 6.60 (dd, $^3J_{H,H}$ = 7.4 Hz, $^4J_{H,H}$ = 1.6 Hz, 1H, H(3)−PhO), 6.78 (t, $^3J_{H,H}$ = 7.4 Hz, 1H, H(4)−PhO), 7.37 (dd, $^3J_{H,H}$ = 7.8 Hz, $^4J_{H,H}$ = 1.8 Hz, 1H, H(5)−PhO). $^{13}C\{^1H\}$ NMR (100 MHz, C_6D_6): δ −11.0 (Al*Me*), 29.7 (C*Me*$_3$), 35.2 (*C*Me$_3$), 43.6 (N*Me*$_2$), 44.8 (N*Me*$_2$), 63.0 (Ph*C*H$_2$), 117.9 (C(4)−PhO), 121.4 (C(2)−PhO), 128.4 (C(3)−PhO), 128.8 (C(5)−PhO), 139.5 (C(6)−PhO), 157.9 (C(1)−PhO). ^{19}F NMR (376 MHz, C_6D_6): δ −120.4 (dd, $^3J_{FF}$ = 23 Hz, $^4J_{FF}$ = 10 Hz, 2F, *o*-C$_6$*F*$_5$), −154.1 (t, $^3J_{FF}$ = 23 Hz, 1F, *p*-C$_6$*F*$_5$), −162.1 (m, 2F, *m*-C$_6$*F*$_5$). Anal. Calcd for $C_{20}H_{23}AlF_5NO$: C, 57.83; H, 5.58. Found: C, 57.50; H, 5.42.

Propylene Oxide Polymerization Procedure. In a glovebox, the catalyst (0.38 mmol) was weighed into a Schlenk tube equipped with a magnetic stirring bar and 2 mL of toluene was added. The tube was taken out of the glovebox, immersed in a temperature-controlled bath, and connected to a N_2 vacuum line. Propylene oxide (2.66 mL, 200 equiv) was then added by syringe. The mixture was then stirred for 15 min at room temperature (or for 1 h when performed at 0 °C) and quenched with methanol (15 mL). The resulting precipitate was filtered through a glass frit and the solvent removed under vacuum to yield an almost colorless viscous liquid, which was analyzed by ^{13}C NMR spectroscopy and by SEC. ^{13}C NMR (200 MHz, $CDCl_3$): δ 75.8−75.0 (*C*H−O), 73.6−72.7 (*C*H$_2$−O), 17.3−17.0 (*C*H$_3$).

X-ray Crystallographic Study. The structure determinations of **2b**,**d**, [**3a**][MeB(C$_6$F$_5$)$_3$], and [**3b**′][MeB(C$_6$F$_5$)$_3$] were carried out on a Nonius Kappa-CCD area detector diffractometer using graphite-monochromated Mo Kα radiation (λ = 0.710 73 Å). The cell parameters were determined from reflections taken from one set of 10 frames (1.0° steps in ψ angle), each at 20 s exposure. The structures were solved using direct methods (SIR97) and refined against F^2 using the SHELXL97 software. The absorption was not corrected. All non-hydrogen atoms were refined anisotropically. Hydrogen atoms were generated according to the stereochemistry and refined using a riding model in SHELXL97. All hydrogen atoms were placed from Fourier difference maps and refined isotropically.

Acknowledgment. We thank the Centre National de la Recherche Scientifique (CNRS) for financial support, A. Decian (University of Strasbourg, France) for X-ray crystallography analysis of **2d**, and M.-N. Rager (ENSCP, Paris, France) for 2D NMR assistance.

Supporting Information Available: Tables giving X-ray crystallographic data for **2b**,**d**, [**3a**][MeB(C$_6$F$_5$)$_3$], and [**3b**′][MeB(C$_6$F$_5$)$_3$]. This material is available free of charge via the Internet at http://pubs.acs.org.

OM0302185